# Kinetic Isotope Effects for the Reactions of Muonic Helium and Muonium with $H_2$

Donald G. Fleming, *et al.*

*Science* **331**, 448 (2011);
DOI: 10.1126/science.1199421

37. F. Matino *et al.*, *Chem. Commun. (Camb.)* **46**, 6780 (2010).
38. R. B. Lauffer, *Chem. Rev.* **87**, 901 (1987).
39. L. Knutsson, F. Ståhlberg, R. Wirestam, *Magn. Reson. Mater. Phys.* **23**, 1 (2010).
40. H. Sugimoto, K. Kuramoto, S. Inoue, *Perkin Trans.* **1**, 1826 (2002).
41. This work was supported by the Deutsche Forschungsgemeinschaft through SFB 677. We thank the Alexander von Humboldt Foundation for a research fellowship for S.V. We are also grateful for support from R. Siewertsen and F. Temps (Institut für Physikalische Chemie, Universität Kiel), G. Peters (Institut für Anorganische Chemie, Universität Kiel), and O. Jansen, C. Riedel and M. Helle (Institut für Neuroradiologie, Universitätsklinikum Schleswig-Holstein). The Christian-Albrechts-Universität zu Kiel and Universitätsklinikum Schleswig-Holstein have filed a patent application for the compound described herein as an MRI contrast agent.

**Supporting Online Material**
www.sciencemag.org/cgi/content/full/331/6016/445/DC1
Materials and Methods
SOM Text
Figs. S1 to S22
Tables S1 to S6
References

2 December 2010; accepted 30 December 2010
10.1126/science.1201180

# Kinetic Isotope Effects for the Reactions of Muonic Helium and Muonium with $H_2$

**Donald G. Fleming,[1]* Donald J. Arseneau,[1] Oleksandr Sukhorukov,[1,2] Jess H. Brewer,[3] Steven L. Mielke,[4] George C. Schatz,[5] Bruce C. Garrett,[6] Kirk A. Peterson,[7] Donald G. Truhlar[4]***

The neutral muonic helium atom may be regarded as the heaviest isotope of the hydrogen atom, with a mass of ~4.1 atomic mass units ($^{4.1}$H), because the negative muon almost perfectly screens one proton charge. We report the reaction rate of $^{4.1}$H with $^{1}H_2$ to produce $^{4.1}H^{1}H + {}^{1}H$ at 295 to 500 kelvin. The experimental rate constants are compared with the predictions of accurate quantum-mechanical dynamics calculations carried out on an accurate Born-Huang potential energy surface and with previously measured rate constants of $^{0.11}$H (where $^{0.11}$H is shorthand for muonium). Kinetic isotope effects can be compared for the unprecedentedly large mass ratio of 36. The agreement with accurate quantum dynamics is quantitative at 500 kelvin, and variational transition-state theory is used to interpret the extremely low (large inverse) kinetic isotope effects in the $10^{-4}$ to $10^{-2}$ range.

Isotopic substitution provides a widely used tool for mechanistic analysis of chemical reaction rates and is a test bed for fundamental theories of chemical kinetics (*1*). A key simplifying assumption in chemical dynamics is the Born-Oppenheimer (BO) approximation (*2*), which allows the potential energy surface (PES) that governs nuclear motion to be calculated independently of the motion of the nuclear masses. The BO approximation facilitates the calculation and interpretation of kinetic isotope effects (KIEs), defined as the ratio of rate constants for two reactions differing only in isotopic masses, which provide mechanistic information even for complex reactions. The largest conventional KIEs are associated with substitution of $^{2}$H or $^{3}$H for $^{1}$H. However, by using muons, one can access KIEs corresponding to isotopic mass ratios much greater than even 3 (*3*–*5*), and here we present an example with the unprecedentedly large ratio of 36.4.

The lightest H atom isotope is muonium (Mu), in which an electron ($e$) orbits a positive muon ($\mu^+$) "nucleus," which is 206 times heavier than an electron, so that Mu [$^{0.11}$H, 0.113 atomic mass units (amu)] behaves chemically like a very light H atom (unlike positronium, for instance). Here we label Mu as $^{0.11}$H to emphasize its importance for kinetics as a pseudo-isotope of H. Because of its light mass, $^{0.11}$H has proven to be an unusually sensitive probe of quantum effects on nuclear motion in reaction rates, both in terms of zero–point-energy (ZPE) shifts and in its propensity to manifest quantum tunneling (*5*, *6*).

In contrast to Mu, the heaviest usable isotope of H can be created by using a negative muon ($\mu^-$) to replace an electron in He to form Heμ, with an atomic mass of 4.116 amu (*7*). Because the muon is much heavier than an electron, its 1*s* orbital is very close to the nucleus (mean radius of 0.2 pm), effectively screening one proton charge, so that Heμ may be considered a virtual isotope of H, and so we will label it $^{4.1}$H as shorthand. [The decimal character of 4.1 is a reminder that this is not a conventional H isotope such as quadrium, $^{4}$H, or other isotopes up to $^{7}$H (*8*), with lifetimes, when known, in the 0.1 to 1 zs range.] Here we report a measurement of the rate constant $k_{4.1}$ for reaction of this heaviest isotope of the H atom with diprotium, and we compare the results with theory.

It has been said (*9*) that "Explaining the $H + H_2$ reaction is without question the most important problem in chemical dynamics. . . . A successful theoretical description is crucial because the credibility of every other theoretical advance in the field rests with the solution to the $H + H_2$ problem." For $^{2}H + {}^{1}H_2$ and $^{1}H + {}^{2}H_2$, theory and experiment converged in 2003 (*10*). Here we report the application of the same theoretical methods to the reactions of $^{4.1}$H and $^{0.11}$H with $^{1}H_2$, along with results for the new experiments on the former. Combining these with previous (*11*) experimental results for the rate constant $k_{0.11}$ for the reaction $^{0.11}H + {}^{1}H_2$ allows a comparison of experiment and theory for this fundamental reaction over a mass ratio of 36.4. The theoretical results are based on an accurate PES and accurate quantum dynamics calculations so that—in contrast to the usual situation—the theoretical results for this system can be used as benchmarks to validate the experimental approach. We also report and compare calculations based on variational transition-state theory (*12*) (VTST); this method is approximate, but testing it is important because of its applicability to complex reactions for which accurate quantum dynamics are impractical (*1*, *13*).

Muon beams can be produced with essentially 100% longitudinal spin polarization at a nuclear

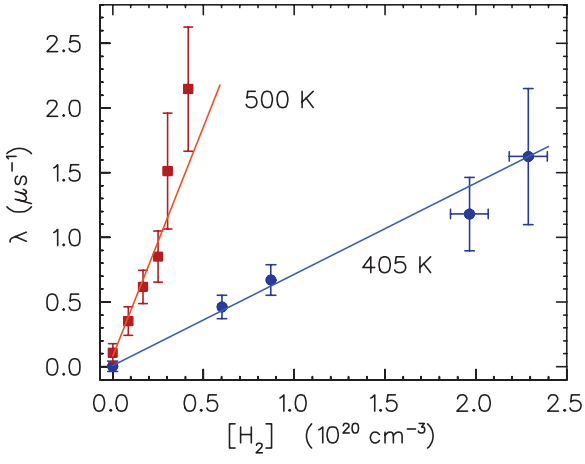


**Fig. 1.** Relaxation rates versus concentration of $H_2$ at 405 K (blue data points and fitted line) and 500 K (red data points and fitted line) at 500 bar of He.

[1]TRIUMF and Department of Chemistry, University of British Columbia, Vancouver, British Columbia, Canada V6T 1Z1. [2]Department of Chemistry, University of Alberta, Edmonton, Alberta, Canada T6G 2G2. [3]Department of Physics, University of British Columbia, Vancouver, British Columbia, Canada V6T 1Z1. [4]Department of Chemistry and Supercomputing Institute, University of Minnesota, Minneapolis, MN 55455–0431, USA. [5]Department of Chemistry, Northwestern University, Evanston, IL 60208–3113, USA. [6]Chemical and Material Sciences Division, Pacific Northwest National Laboratory, Richland, WA 99352, USA. [7]Department of Chemistry, Washington State University, Pullman, WA 99164–4630, USA.

*To whom correspondence should be addressed. E-mail: flem@triumf.ca (D.G.F.); truhlar@umn.edu (D.G.T.)

accelerator such as TRIUMF, where the present experiments with negative muons ($\mu^-$) were carried out. In the decay of the muon ($\mu^- \rightarrow e^- \bar{\nu}_e \nu_\mu$), the resulting electron, which is detected in the experiments, is emitted preferentially opposite to the muon spin direction [see the supporting online material (SOM) (*14*)]. In a low transverse magnetic field, a fixed counter in the plane of precession will detect an oscillating signal with a characteristic Larmor frequency as the muon spin sweeps past its solid angle (*15*); this is the basis of the transverse-field muon spin rotation technique (*16*) we used.

Although the kinetic energies of muons are several million electron volts upon entering the gas target, most of this energy is lost to ionization and inelastic scattering processes down to energies of ~100 keV (*16*); there is no loss in muon spin polarization because the muon spin is unaffected by these Coulomb interaction processes. At lower energies, the $\mu^-$ is captured into a muonic orbit by He, which ejects both of its electrons, leaving the $^{4.1}H^+$ ion, which is neutralized in a charge-exchange collision (*15*) with ammonia dopant.

The experimental data are in histograms of the time differences between the detection of an incoming muon and the detection of its electron decay product. Superimposed on the signal is a function that reflects the interaction of the spin-polarized muon with its environment. Any process that causes a spin flip or spin dephasing causes a relaxation of the signal, with relaxation rate λ; the most important process here is the pseudo–first-order reaction of $^{4.1}H$ with $H_2$. The procedure for analyzing the data is presented elsewhere (*7*), and further experimental details are given in the SOM (*14*). Examples of the measured relaxation rates are in Fig. 1.

For high accuracy, the present calculations replace the usual BO PES with the Born-Huang (*17*) PES. The latter is obtained by adding the BO diagonal correction, which depends on nuclear masses. The BO surface (*18*) is a fit to essentially complete configuration interaction calculations. The diagonal correction (*19*) raises the BO barrier of 9.60 kcal/mol to 9.73 for $^{4.1}He$ and to 9.97 for $^{0.11}H$.

The quantum-dynamics calculations used the outgoing wave variational principle (*20*), numerically converged to better than 1%. The VTST calculations were carried out by improved canonical variational theory (ICVT) (*21*), with least-action ground-state (LAG) multidimensional tunneling contributions (*22*), and with the bound stretching vibration treated with the Wentzel-Kramers-Brillouin approximation (*23*) and bends treated with the centrifugal oscillator approximation (*24*).

The rate constants, $k_{4.1}$, determined from the slopes of plots such as those in Fig. 1, are shown in the Arrhenius plot of Fig. 2, where they are compared to theory. The VTST results are shown both with (ICVT/LAG) and without (ICVT) tunneling (both VTST results include ZPE); comparison of these results shows that tunneling makes a large contribution to the rate. The accurate quantum-mechanical (QM) calculations are in excellent agreement with the experimental data at 500 and 405 K, where they are well within experimental error, but the calculated rates are below experimental values at 295 K by 30%, a surprisingly large disagreement. Possible systematic errors that could be more important at the lowest temperature (where the rate is smallest) are impurities in the $H_2$ or additional relaxation caused by nonreactive collisions. The ICVT/LAG calculations of $k_{4.1}$ are consistently below both accurate QM theory and experiment at all temperatures, although they agree with the QM results within 23% over the temperature range plotted. The largest uncertainties in the ICVT/LAG calculations are in the tunneling contributions.

The present experimental results for the reaction rate of the heaviest H-atom isotope, muonic He, with the protium molecule can now be compared with that for the lightest H-atom isotope, muonium, corresponding to an unprecedented factor of 36.4 in atomic mass. The ratio of rate constants is given in Fig. 3, which contains only one experimental point because the $^{0.11}H + {}^1H_2$ experiments (*11*) extend down only to 473 K. The usual convention is to place the rate constant for the lighter isotope in the numerator, because that yields a normal KIE greater than 1. The present KIE defined this way, $k_{0.11}/k_{4.1}$, however, is inverse (less than 1) and strikingly small, with an experimental value of 0.0108 and an accurate quantum value of 0.0104 at 500 K. The finding that accurate quantum dynamics agrees essentially perfectly with experiment, even though the KIE is a very strong function of temperature (Fig. 3), argues convincingly that $^{4.1}H$ is indeed a H isotope, and nothing (such as geometric phases or nonadiabatic behavior) beyond a nonrelativistic treatment of single–potential-energy-surface scattering on the Born-Huang surface needs to be considered. This result is a dramatic confirmation of the success of quantum scattering calculations and the experiments in a difficult arena. When the temperature is lowered, the accurate quantum scattering result becomes $2.46 \times 10^{-3}$ at 405 K and $1.74 \times 10^{-4}$ at 295 K, with the latter being (to our knowledge) the smallest KIE ever reported.

Conventional transition-state theory without tunneling, which is widely used to interpret reaction mechanisms (*25*), predicts a KIE of 1/19 at 500 K, in contrast to 1/90 by ICVT/LAG and the accurate value of 1/96. The good agreement of VTST calculations with accurate quantum results allows them to be used to assess vibrational contributions at the transition state and the importance of quantum tunneling, neither of which is explicit in the fully quantum calculations. The VTST calculations show that the large inverse KIE may be attributed primarily to the difference in stretching-vibration ZPE at the two transition states (the two reactions have identical reactant ZPEs). At their respective variational transition states at 500 K, the $^{4.1}He$ reaction has a ZPE of 5.3 kcal/mol (2.9 in stretch and 2.4 in bend), whereas the $^{0.11}H$ reaction has a ZPE of 13.8 kcal/mol (9.8 in stretch and 4.0 in bend). The good agreement

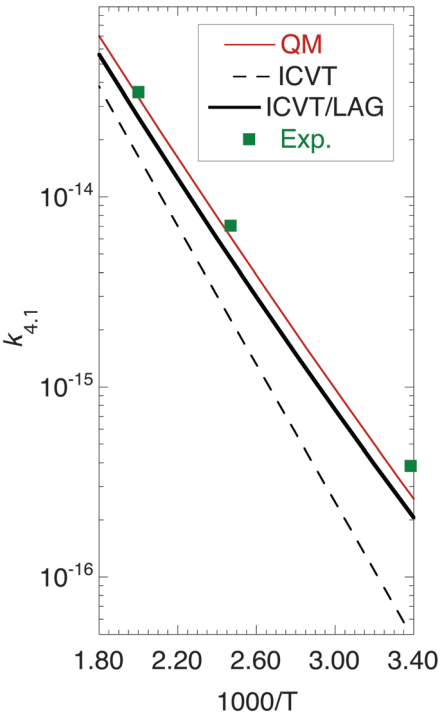


**Fig. 2.** Comparison of experimental and theoretical thermal rate constants of the $^{4.1}H + {}^1H_2$ reaction (in units of cubic centimeters per molecule per second).

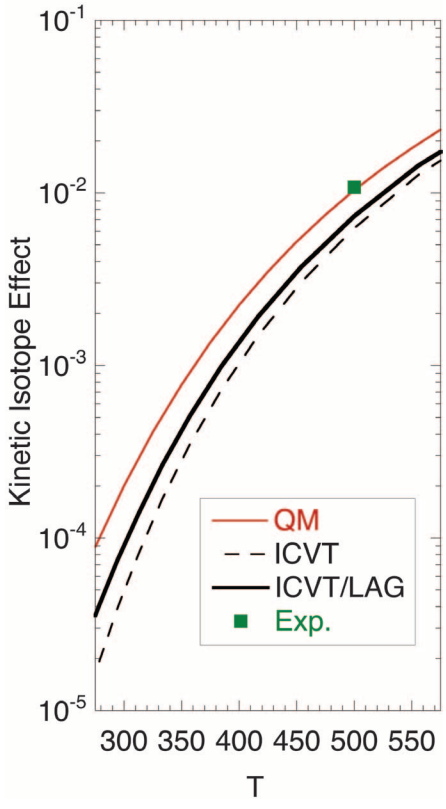


**Fig. 3.** Comparison of experimental and theoretical kinetic isotope effects ($k_{0.11}/k_{4.1}$). The experimental point was obtained using the published experimental fit for the $^{0.11}H$ reaction and the experimental datum at 500 K for the $^{4.1}H$ reaction.

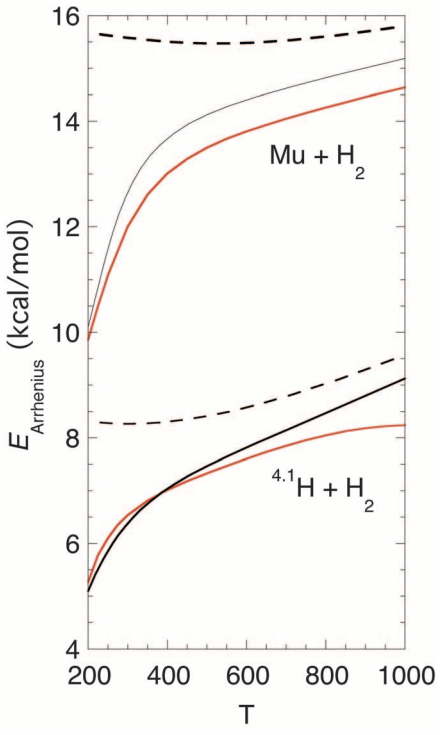


**Fig. 4.** Comparison of Arrhenius activation energies ($E_a \equiv E_{Arrhenius}$) calculated via QM (red solid lines), ICVT (dashed black lines), and ICVT/LAG (solid black lines) for the reactions of $^{4.1}$H and $^{0.11}$H with $H_2$ as a function of temperature ($T$).

(within 23%) of the VTST calculations with experiment lends credence to the existence of quantized transition states (*26*, *27*) with these large amounts of vibrational energy.

The tunneling transmission coefficient, which is the ratio of the ICVT/LAG rate constant to the ICVT rate constant, is 4.3, 2.1, and 1.6 at 295, 405, and 500 K, respectively. Reactions of $^{0.11}$H may exhibit greater tunneling effects than heavier isotopes because of the small mass (*6*), and this would be true in any one-dimensional treatment with an isotope-independent effective barrier. However, the LAG approximation is multidimensional, including ZPE effects (*28*, *29*) in the effective tunneling barriers and isotope-dependent tunneling paths, and the effective barrier to tunneling is much broader for the $^{0.11}$H case because of the large ZPE of the $^{0.11}$H$^{1}$H product (*30*). It is very encouraging that the results based on the LAG tunneling treatment, which is affordable for complex systems (*31*), correctly accounts for the KIE despite the quite different effective potentials for the two isotopes, confirming the physicality of the isotope-dependent barriers.

The Arrhenius (*32*) activation energy is defined as

$$E_a = -R\frac{d\ \ln\ k}{d(1/T)} \qquad (1)$$

which is proportional to the negative slope of an Arrhenius plot. It is well known (*33*, *34*) that $E_a$ can exhibit substantial temperature dependence, and the present reactions illustrate this in Fig. 4; this kind of detail cannot be revealed yet by experiment. Figure 4 shows that $E_a$ would be quite different in magnitude and temperature dependence without tunneling, but with tunneling, the ICVT/LAG calculation agrees very well with the dramatic temperature dependence and isotope dependence shown by the accurate quantum-dynamical results. These results confirm the usefulness of VTST for interpreting large quantum effects.

### References and Notes


1. A Kohen, H.-H. Limbach, Eds., *Isotope Effects in Chemistry and Biology* (Taylor & Francis, Boca Raton, FL, 2006).
2. M. Born, J. R. Oppenheimer, *Ann. Phys.* **84**, 457 (1927).
3. J. Espinosa-Garcia, *Phys. Chem. Chem. Phys.* **10**, 1277 (2008).
4. D. C. Walker, *J. Phys. Chem.* **85**, 3960 (1981).
5. S. Baer *et al.*, *ACS Symp. Ser.* **502**, 111 (1992).
6. T. Tanaka, T. Takayanagi, *Chem. Phys. Lett.* **496**, 248 (2010).
7. D. J. Arseneau *et al.*, *Physica B* **404**, 946 (2009).
8. G. Audi *et al.*, *Nucl. Phys. A.* **729**, 3 (2003).
9. J. V. Michael, K. P. Lim, *Annu. Rev. Phys. Chem.* **44**, 429 (1993).
10. S. L. Mielke *et al.*, *Phys. Rev. Lett.* **91**, 063201 (2003).
11. I. D. Reid *et al.*, *J. Chem. Phys.* **86**, 5578 (1987).
12. D. G. Truhlar, B. C. Garrett, *Acc. Chem. Res.* **13**, 440 (1980).
13. A. Dybala-Defratyka, P. Paneth, R. Banerjee, D. G. Truhlar, *Proc. Natl. Acad. Sci. U.S.A.* **104**, 10774 (2007).
14. Experimental details, including scheme S1, are in the SOM on *Science* Online.
15. P. A. Souder *et al.*, *Phys. Rev. A* **22**, 33 (1980).
16. M. Senba *et al.*, *Phys. Rev. A* **74**, 042708 (2006).
17. M. Born, K. Huang, *The Dynamical Theory of Crystal Lattices* (Oxford Univ. Press, London, 1954).
18. S. L. Mielke, B. C. Garrett, K. A. Peterson, *J. Chem. Phys.* **116**, 4142 (2002).
19. S. L. Mielke, D. W. Schwenke, G. C. Schatz, B. C. Garrett, K. A. Peterson, *J. Phys. Chem. A* **113**, 4479 (2009).
20. Y. Sun *et al.*, *Phys. Rev. A* **41**, 4857 (1990).
21. B. C. Garrett, D. G. Truhlar, R. S. Grev, A. W. Magnusson, *J. Phys. Chem.* **84**, 1730 (1980).
22. B. C. Garrett, D. G. Truhlar, *J. Phys. Chem.* **79**, 4931 (1983).
23. B. C. Garrett, D. G. Truhlar, *J. Chem. Phys.* **81**, 309 (1984).
24. B. C. Garrett, D. G. Truhlar, *J. Phys. Chem.* **95**, 10374 (1991).
25. C. F. Bernasconi, Ed., *Investigation of Rates and Mechanisms of Reactions* (Wiley, New York, ed. 4, 1986).
26. D. C. Chatfield, R. S. Friedman, D. G. Truhlar, D. W. Schwenke, *Faraday Discuss. Chem. Soc.* **91**, 289 (1991).
27. D. C. Chatfield, R. S. Friedman, D. W. Schwenke, D. G. Truhlar, *J. Phys. Chem.* **96**, 2414 (1992).
28. R. A. Marcus, *J. Chem. Phys.* **41**, 610 (1964).
29. A. Kuppermann, D. G. Truhlar, *J. Am. Chem. Soc.* **93**, 1840 (1971).
30. B. C. Garrett *et al.*, *Hyperfine Interact.* **32**, 779 (1986).
31. R. Meana-Pañeda, D. G. Truhlar, A. Fernández-Ramos, *J. Chem. Theory Comput.* **6**, 6 (2010).
32. S. Arrhenius, *Z. Physikal. Chem* **4**, 226 (1889).
33. N. C. Blais *et al.*, *J. Phys. Chem.* **85**, 1094 (1981).
34. B. C. Garrett *et al.*, *J. Am. Chem. Soc.* **108**, 3515 (1986).


35. We thank the Natural Sciences and Engineering Research Council of Canada, the Office of Basic Energy Sciences of the U.S. Department of Energy (DOE), and the Air Force Office of Scientific Research for their support of this work. Battelle operates the Pacific Northwest National Laboratory for DOE.


### Supporting Online Material

www.sciencemag.org/cgi/content/full/331/6016/448/DC1
Methods
Scheme S1
References

22 October 2010; accepted 7 December 2010
10.1126/science.1199421



# Enhanced Modern Heat Transfer to the Arctic by Warm Atlantic Water

**Robert F. Spielhagen,[1,2]* Kirstin Werner,[2] Steffen Aagaard Sørensen,[3] Katarzyna Zamelczyk,[3] Evguenia Kandiano,[2] Gereon Budeus,[4] Katrine Husum,[3] Thomas M. Marchitto,[5] Morten Hald[3]**

The Arctic is responding more rapidly to global warming than most other areas on our planet. Northward-flowing Atlantic Water is the major means of heat advection toward the Arctic and strongly affects the sea ice distribution. Records of its natural variability are critical for the understanding of feedback mechanisms and the future of the Arctic climate system, but continuous historical records reach back only ~150 years. Here, we present a multidecadal-scale record of ocean temperature variations during the past 2000 years, derived from marine sediments off Western Svalbard (79°N). We find that early–21st-century temperatures of Atlantic Water entering the Arctic Ocean are unprecedented over the past 2000 years and are presumably linked to the Arctic amplification of global warming.

Rising air temperatures (*1*–*3*) and a decline of the sea ice cover (*4*, *5*) evidence a rapid warming in the Arctic that has reversed a long-term cooling trend (*6*). Relatively warm Atlantic Water (AW) in the Fram Strait Branch (FSB) of the North Atlantic Current is the major carrier of oceanic heat to the Arctic Ocean (Fig. 1). It maintains perennially ice-free conditions in the eastern Fram Strait today and supplies salt to the intermediate and bottom waters of the Arctic Ocean, thereby stabilizing the stratification (*7*, *8*). In the eastern Fram Strait, AW with temperatures of 2° to 6°C and salinities of >35.0 is found at 50- to 600-m water depth (Fig. 2). Most of the year it is overlain by a mixed layer of lower salinity, seasonally variable temperatures, and ice coverage in ex-

[1]Academy of Sciences, Humanities, and Literature, 53151 Mainz, Germany. [2]Leibniz Institute of Marine Sciences (IFM-GEOMAR), 24148 Kiel, Germany. [3]Department of Geology, University of Tromsø, 9037 Tromsø, Norway. [4]Alfred Wegener Institute of Polar and Marine Research, 27515 Bremerhaven, Germany. [5]Department of Geological Sciences and Institute of Arctic and Alpine Research, University of Colorado, Boulder, CO 80309, USA.

*E-mail: rspielhagen@ifm-geomar.de